MECHANISMS OF RADICAL REMOVAL BY SO_2

Christian Lund Rasmussen[1], Peter Glarborg[1], Paul Marshall[2]

[1] *Department of Chemical Engineering, Technical University of Denmark, DK-2800 Kgs. Lyngby, Denmark*
[2] *Department of Chemistry, University of North Texas, Denton, Texas 76203-5070*

Abstract

It is well established from experiments in premixed, laminar flames, jet-stirred reactors, flow reactors, and batch reactors that SO_2 acts to catalyze hydrogen atom removal at stoichiometric and reducing conditions. However, the commonly accepted mechanism for radical removal, $SO_2 + H(+M) \rightleftharpoons HOSO(+M)$, $HOSO + H/OH \rightleftharpoons SO_2 + H_2/H_2O$, has been challenged by recent theoretical and experimental results. Based on *ab initio* calculations for key reactions, we update the kinetic model for this chemistry and re-examine the mechanism of fuel/SO_2 interactions. We find that the interaction of SO_2 with the radical pool is more complex than previously assumed, involving HOSO and SO, as well as, at high temperatures also HSO, SH and S. The revised mechanism with a high rate constant for H+SO_2 recombination and with SO+H_2O, rather than SO_2+H_2, as major products of the HOSO+H reaction is in agreement with a range of experimental results from batch and flow reactors, as well as laminar flames.

Keywords: sulfur chemistry, inhibition, kinetics

1. Introduction

The presence of SO_2 has been reported to catalyze H atom removal at medium to high temperatures in rich, premixed laminar flames [1, 2, 3, 4, 5, 6, 7] and laboratory reactors [8, 9]. The mechanism for radical removal is commonly recognized to be of the type, X+SO_2+M→XSO_2+M, Y+XSO_2→XY+SO_2, where X and Y may be H, O, or OH. The most important radical removal cycle under stoichiometric and reducing conditions is believed to be initiated by recombination of SO_2 with H to form an H/SO_2 adduct

$$SO_2 + H + M \rightleftharpoons H/SO_2 + M$$

followed by recycling of this adduct to SO_2 by reaction with H or OH. The H/SO_2 adduct is most likely HOSO, which is thermally more stable than the HSO_2 isomer,

$$SO_2 + H(+M) \rightleftharpoons HOSO(+M) \qquad \text{(R9)}$$

$$HOSO + H \rightleftharpoons SO_2 + H_2 \qquad \text{(R27)}$$

$$HOSO + OH \rightleftharpoons SO_2 + H_2O \qquad \text{(R29)}$$

The reaction numbers refer to the listing in Table 1. This sequence of reactions has been proposed to be the principal radical sink in fuel-rich flames doped

with SO_2 [2, 5, 7]. However, due to uncertainty in the H+SO_2 reaction rate and in the fate of the HOSO intermediate, the mechanism of inhibition is still in question. There are no direct measurements of the H+SO_2 recombination rate at high temperatures. Theoretical work [10, 11, 12] as well as values deduced from flames [13], batch reactor [8], and flow reactor experiments [9] imply that the reaction is comparatively fast, while other experimental results indicate a much slower reaction [14]. Regarding HOSO, recent theoretical investigations of the HOSO+H reaction [15] indicate that SO+H_2O, and not SO_2+H_2, is the major product channel. Hence,

$$\mathrm{HOSO + H \rightleftharpoons {}^1SO + H_2O} \qquad \text{(R26)}$$

In the ground state SO is a triplet (^{3}SO), but in reaction (R26) it is formed in the singlet state. Both ^{1}SO and ^{3}SO are reactive towards O_2 to make SO_2+O in which case, the HOSO+H reaction becomes chain propagating rather than terminating and the efficiency of the radical removal cycle decreases.

The objective of the present work is to re-examine the interaction of SO_2 with the radical pool at atmospheric pressure under stoichiometric and fuel-rich combustion conditions. The H/S/O reaction mechanism is updated and a number of key reactions are analyzed. Modeling predictions are compared with experimental results from a batch reactor [8], flow reactors [9, 14] and laminar flames [5] for oxidation of H_2 and/or CO doped with SO_2, and the mechanisms of inhibition are discussed.

2. Reaction Mechanism

The proposed reaction mechanism consists of a description of the CO/H_2 oxidation system and a subset describing sulfur reactions. The thermochemistry was mostly adopted from previous modeling studies [14, 16], except for HOSO/HSO_2 [10], and $HOSO_2$ [17]. For the singlet SO species introduced in the present mechanism, we have estimated a heat of formation of $\Delta_f H_{298}$ = 23.90 kcal/mol and an entropy of S_{298} = 50.89 cal/mol·K. From *ab initio* calculations [18] the excitation energy for the first singlet state was estimated to 22.4 kcal/mol. This value is somewhat higher than the estimate from Huber and Herzberg [19] of 18.1 kcal/mol, but it is in agreement with the corresponding value for O_2 (22.7 kcal/mol).

The sulfur reaction chemistry was mainly adopted from Alzueta et al. [14]. However, a number of rate constants were modified according to *ab initio* calculations [18], and the S_2H_x subset was updated with data from Sendt et al. [20]. Data for some important reactions in the sulfur subset are found in Table 1.

Interactions between SO_2 and the radical pool are primarily facilitated by recombination with H (R9, R10) and to a lesser extent O (R11). Recombination of SO_2 with OH is not important under the conditions of interest in this study due to the low thermal stability of $HOSO_2$ [17]. There are no direct measurements of the SO_2+H(+M) recombination reaction at high temperatures, but theoretical estimates are in fairly good agreement [10, 11, 12]. We have adopted the rate constants for formation of HOSO (R9) and HSO_2 (R10) from the recent work of Blitz et al. [12]. The recombination of H and SO_2 competes with the reaction SO_2+H⇌SO+OH (–R3), which is now well characterized over a wide temperature range [21, 32]. The rate coefficients for the recombination of SO_2 with O to form SO_3 were drawn from recent work by the authors [23, 24].

The key reactions of HOSO are those with H (R26, R27), OH (R29) and O_2 (R28). A recent *ab initio* study [15, 18] of the HOSO+H reaction indicates a very fast reaction yielding >95 % ^{1}SO+H_2O (R26) following an addition/elimination mechanism. Formation of SO in the singlet state conserves spin; however it is possible that intersystem crossing occurs during the course of reaction (R26) and that the triplet state occurs directly. The alternative abstraction channel to SO_2+H_2 (R27) is significantly slower due to a bottleneck along the reaction coordinate. The HOSO+OH reaction (R29) could be abstraction or addition/elimination that either way leads to SO_2+H_2O. We expect this reaction to proceed without a barrier.

In previous modeling work [9, 14] the rate constant for the HOSO+O_2 reaction (R28) was adopted from the work of Lovejoy et al. [33]. However, in their work the H/SO_2 isomer was formed from the reaction of HSO with NO_2. This reaction is likely to form HSO_2 rather than HOSO and for this reason their measurements are expected to apply to the HSO_2+O_2 reaction rather than HOSO+O_2. The HOSO+O_2 reaction is a system where both reactants and products can hydrogen bond (by about 5–6 kcal/mol) and we estimate the H-transfer barrier between the two complexes to be modest. Consequently, we expect no overall energy barrier for this exothermic process, which is in agreement with the recent theoretical study by Wang and Hou [34]. Wang and Hou estimate the reaction to be very fast due to an "outer" transition state that leads into an initial adduct. However, the formation of this transition state is only rate limiting at low temperatures. At elevated temperatures an "inner" transition state containing a tight entropy bottleneck comes into play. From *ab initio* calculations [18] we estimate the 1000–1500 K rate constant to be of the order of 10^{11} cm^3/mol·s and decreasing with temperature. These values were obtained from a simple transition state theory approach and are expected to represent an upper limit.

The SO formed in reaction (R26) is in the singlet state if spin is conserved [15]. It would be expected that ^{1}SO is more reactive than the ground triplet state ^{3}SO. However, under the dilute conditions of interest here (see below), ^{1}SO is mostly quenched to the ground state, even though a fraction may react with O_2. We have estimated a rate for the collisional intersystem crossing (R7) of 10^{13} cm^3/mol·s. Modeling results are not sensitive to this value. Reactions with H_2 and H_2O were included in the mechanism, but they

are too endothermic to gain importance. The reaction of ^{3}SO with O_2 (R5) is well characterized experimentally [14]. This is not the case for the reaction of ^{3}SO with HO_2 (R6), but *ab initio* calculations [18] indicate that this reaction is relatively fast and proceeds without barriers. Recombination of SO with H atoms is a potential radical sink [14], but according to *ab initio* calculations [18] the reaction is slow. The present estimate is in good agreement with estimates previously used in modeling [14].

3. Results and Discussion

For validation of the kinetic model, calculations were compared with experimental data on the effect of SO_2 addition on oxidation of H_2 and/or CO in a batch reactor [8], flow reactors [9, 14] and laminar premixed flames [5]. The flow reactor data were obtained in laminar flow reactors designed to approximate plug flow and the data were modeled with SENKIN [35] from the CHEMKIN library [36]. SENKIN performs an integration in time. The results from the SENKIN calculations were compared to experimental data using the nominal residence time in the reactor. The batch reactor and flame data were also simulated with SENKIN, as discussed below.

3.1. Batch Reactor Results

We first consider a series of batch reactor experiments [8] where the inhibiting effect of SO_2 addition on the H_2/O_2 reaction at the second pressure limit of explosion is investigated at 784 K. Pure H_2, O_2 and SO_2 were premixed in specific ratios at a pressure greater than the second explosion limit. Gases were then withdrawn from the vessel until explosion occurred [8]. These conditions are modeled as an adiabatic batch reactor (SENKIN) where a temperature increase >100 K within a reactor residence time of 0.1 sec constitutes the criterion of explosion. The second pressure limit of explosion is governed by the OH formation reactions: $H+O_2 \rightleftharpoons O+OH$ and $O+H_2 \rightleftharpoons H+OH$. Termination occurs via $H+O_2(+M) \rightleftharpoons HO_2(+M)$ and subsequent loss of HO_2 at the surface. The latter has been accounted for in the mechanism by the reaction $HO_2 \rightarrow wall$ with a fitted rate constant of 10^7 s^{-1}. It has been necessary to extend the loss of H atoms at the surface by enhancing the third-body efficiencies of the main components H_2 and O_2 in the reaction $H+O_2(+M) \rightleftharpoons HO_2(+M)$ until experimental and numerical predictions match each other at zero SO_2 addition. The resulting third-body efficiencies are 3.3 and 1.29 for H_2 and O_2 respectively, which is 65 % increase from the original values [37].

Figure 1 shows a satisfactory agreement between model predictions and measurements of the second pressure limit as a function of SO_2 concentration at four different H_2/O_2 mixing ratios. Webster and Walsh [8] attributed the observed reduction of the pressure limit to H atom removal by the SO_2+H(+M) recombination reaction (R9). This is confirmed by a sensitivity analysis that identifies (R9) as the single most important bottleneck in the sulphur conversion network at all four mixing ratios. Hence, at the pressure limit of explosion and a mixing ratio of $H_2/O_2 = 1/3$, the first order sensitivity coefficient of (R9) yields a magnitude of about 15-20 % of the sensitivity coefficient of the most important reaction in the system; $H+O_2 \rightleftharpoons O+OH$. This value increases to about 25-30 % when $H_2/O_2 = 3/2$.

Webster and Walsh estimated that the rate constant of (R9) at 784 K had to be 2.0 times the rate constant of reaction $H+O_2(+M) \rightleftharpoons HO_2(+M)$ to match the observed reduction of the pressure limit. In the proposed mechanism k_9 is only ~ 0.4 times this value. However, the satisfactory agreement between experimental and numerical data supports the present rate constant.

3.2. Flow Reactor Results

Laboratory reactor experiments show apparently conflicting results on the effect of SO_2 on CO or CO/H_2 oxidation at intermediate temperatures. Results from jet-stirred reactors and flow reactors under stoichiometric and fuel–rich conditions [9] support the observation from flames that SO_2 has a strong potential for removing radicals. However, other flow reactor experiments [14] conducted at similar stoichiometries and similar SO_2 levels, but with much lower fuel/oxidizer concentrations, show no evidence for the H removal cycle. As a result, the two studies provide recommendations for the value of k_9 that differ by more than an order of magnitude [9, 14]. In the present study, we compare modeling predictions to flow reactor data from both these studies.

Flow reactor results [9] from CO/H_2 oxidation in the presence and absence of SO_2 are compared with model predictions in Fig. 2 and 3 under stoichiometric and fuel-rich conditions, respectively. In the model, loss of radicals on the quartz surface was taken into account through a first-order hydrogen loss reaction [9]. In both cases, the presence of SO_2 causes a considerable inhibition of the fuel oxidation. The fact that the experimental results can be modeled satisfactory with a lower rate constant for the SO_2+H(+M) reaction (R9) than advocated by Dagaut et al. [9] and with the HOSO+H reaction now being chain propagating rather than chain terminating is partly due to the lower present rate constant for $HOSO+O_2$. The interaction of SO_2 with the radical pool is discussed later.

Figure 4 compares modeling predictions with flow reactor data from Alzueta et al. [14]. These data were obtained under fuel-rich conditions, with SO_2 levels similar to those of Fig. 3, but with CO as fuel, and fuel and oxygen concentrations about two orders of magnitude lower. While the experimental data indicate little inhibiting effect of SO_2 under these conditions, the modeling predictions show a considerable effect

and overestimate the onset temperature for rapid oxidation of CO by more than 100 K after which, it underpredicts the fuel conversion rate. We have currently no explanation for this discrepancy. Apparently, there is a chain branching mechanism active for the conditions of Fig. 4, which is less important at high fuel/oxidizer concentrations. Perhaps the high SO_2 level combined with low fuel and oxidizer levels enhance the impact of surface reactions in the reactor; sulfur species are known to be very active on surfaces [38].

3.3. Flame Results

Following Alzueta et al. [14], we take a closer look at the flame data of Kallend [5]. Measured H atom concentration profiles in the post-flame zone of SO_2 doped premixed $H_2/O_2/N_2$ flames have been used to estimate rate constants for both the SO_2+H(+M) recombination reaction (R9) and the subsequent conversion of HOSO by H and OH [13]. It was found that at lower temperatures (<1720 K) removal of H atoms was first order, consistent with reaction (R9) being rate determining, while it was second order at high temperatures (>2000 K).

This was interpreted in terms of partial equilibration of reaction (R9), causing the HOSO consumption steps to determine the rate of the reaction cycle [5]. However, rate constant derivation requires well-defined conditions as well as negligible interference from side-reactions that are not characterized with considerable accuracy. The latter is rarely satisfied in complex high temperature reaction systems like flames and the present data are no exception.

Figure 5 shows comparisons between calculated and measured downstream H atom concentration profiles from three SO_2 doped and one undoped flame with temperatures of 1695, 1980 and 2115 K [5]. Following Alzueta et al. [14], we have modeled these flames assuming plug flow, which is reasonable since temperature and concentration gradients are small in the post-flame region. Despite the changes made in the present model, such as making HOSO+H chain-propagating rather than terminating, all flames show satisfactory agreement between experiments and numerical predictions. Consistent with the previous discussion [14], we find that the sensitivity of sulphur reactions decrease with increasing temperature as recombination reactions in the O/H radical pool, such as H+H(+M) and H+OH, with H_2O as the predominant third-body collision partner, provide an increasingly dominant H atom sink with the temperature.

3.4. Sulphur Catalyzed Radical Decay

According to the present calculations, the interaction of SO_2 with the radical pool is quite complex and involves several chain sequences where characteristic sulphur compounds are recirculated in ways that facilitate a net termination of chain carrying radicals. These cyclic mechanisms are shown together in Fig. 6. However, their fractional contributions to the sulphur flux are very dependent on the reaction conditions.

SO_2 is largely consumed by recombination with H atoms (R9) forming HOSO, which also reacts mainly with H (R26). The competing H atom addition/elimination reaction (–R3) yielding ^{3}SO+OH, mainly operates as a ^{3}SO sink via (R3); as indicated in Fig. 6. However, at high temperatures (>1700 K) the sulphur flux is initially reversed and (–R3) becomes the dominating SO_2 consumption channel. The recombination reaction (R9) eventually takes over as the main SO_2 sink after which, the sulphur flux through (R3) becomes the main SO_2 formation channel. This behavior is not strongly affected by the reaction stoichiometry, whereas increasing temperature promotes the flux through (–R3) and at temperatures roughly above 1900 K, this SO_2 drain predominates throughout most of the fuel conversion.

The ^{3}SO+OH addition/elimination reaction (R3) in sequence (D) competes with the corresponding addition reaction ^{3}SO+OH(+M) (R4) from sequence (C). At lower temperatures (<1500 K) and atmospheric pressure, $\frac{(D)}{(C)} \approx 3$ to 4, but this ratio decreases with increasing temperature until (C)>(D) around 1900 K. This competition between (C) and (D) is very sensitive to the pressure whereas the reaction stoichiometry has little influence.

Sequence (A) and (B) involve conversion of ^{3}SO and HOSO, respectively, by molecular oxygen. These two reactions are most important under fuel-rich conditions, low temperatures and high SO_2 concentrations. These conditions serve to suppress the main OH formation reactions ($H+O_2 \rightleftharpoons O+OH$ and $O+H_2 \rightleftharpoons H+OH$). They are partly obtained in the lower temperature range of the flow reactor experiments in Fig. 2 and 3, where mechanism (A) and (B) govern the main sulphur conversion. However, calculations indicate that mechanism (B) quickly vanishes from the reaction network as the temperature rises above 1000 K.

Sequence (A) also plays a minor role in the batch reactor experiments in Fig. 1. The substantial heat release at the time of the explosion combined with the high availability of oxygen promote the OH formation reactions and make sequence (D) the dominating sulphur conversion mechanism. However, flux analysis reveal that the SO pool is also subjected to a minor drain via mechanism (A), which is facilitated by the high absolute concentration of molecular oxygen. It is noteworthy that a significant part of this drain is facilitated by reaction (R8) where singlet state ^{1}SO is the reactant. A rough determination of the ratio between the two mechanisms indicates a decrease from $\frac{(D)}{(A)} \approx 4.5$ to 2.5 when the mixing ratio in the explosion experiments changes from $\frac{H_2}{O_2} = 3/2$ to 1/3.

H atom addition to ^{3}SO (R1), forming HSO, is only important at high temperatures (>1500 K). Consequently, sequence (E)–(G) only play a significant role in the flame experiments. The ratio $\frac{(C+D)}{(E+F+G)}$ is roughly 1/1 in all the doped flames. The reaction

SH+O (E) only contributes significantly in the 1979 and 2115 K flames, whereas (F) and (G) predominate in the 1695 K flame. High temperatures favor formation of S over SH from HSO, which makes (F)>(E+G) in the 2115 K flame. However, since the increasing flame temperature also favors the pure O/H radical recombination reactions, the effect of the sulphur catalyzed H atom decay gradually diminishes in this temperature range.

Alzueta et al. [14] proposed that S_2 sulfur species might play a role for radical removal in these flames. However, according to our present understanding of the S_2 chemistry [20] and the H/S/O interactions discussed in this work, the S_2 species have only little impact on the radical pool.

4. Conclusions

Based on recent theoretical results for key reactions, the kinetic model for the H/S/O chemistry has been revised and the mechanism of fuel/SO_2 interaction has been re-examined. It is shown that the interaction of SO_2 with the radical pool is more complex than previously assumed, involving HOSO and SO, as well as, at high temperatures also HSO, SH and S. The revised mechanism with a high rate constant for H+SO_2 recombination to HOSO, and with SO+H_2O, rather than SO_2+H_2, as major products of the HOSO+H reaction, is in agreement with a range of experimental results from batch and flow reactors to laminar flames.

Acknowledgments

CLR and PG acknowledge support from the CHEC (Combustion and Harmful Emission Control) Research Program and from PSO-Elkraft (Grant FU-2207). PM thanks the National Science Foundation (Grant CTS-0113605), the Robert A. Welch Foundation (Grant B-1174) and the UNT Faculty Research Fund.

References

[1] Fenimore, C.P. and Jones, G.W. *J. Phys. Chem.* 69:3593-3597 (1965)
[2] Halstead, C.J. and Jenkins, D.R. *Trans. Faraday Soc.* 65:3013–3022 (1969)
[3] Kallend, A.S., *Combust. Flame* 13:324 (1969).
[4] Durie, R.A., Johnson, G.M., and Smith, M.Y. *Combust. Flame* 17:197-203 (1971)
[5] Kallend, A.S., *Combust. Flame* 19:227–236 (1972)
[6] Smith, O.I., Wang, S.-N., Tseregounis, S., and Westbrook, C.K., *Combust. Sci. Techn.* 30:241 (1983)
[7] Zachariah, M.R. and Smith, O.I., *Combust. Flame* 69:125 (1987)
[8] Webster, P., Walsh, A.D., *Proc. Combust. Inst.* 10:463-472 (1965)
[9] Dagaut, P., Lecomte, F., Mieritz, J., and Glarborg, P., *Int. J. Chem. Kin.* 35:564-575 (2003)
[10] Goumri, A., Rocha, J.-D.R., Laakso, D., Smith, C.E., and Marshall, P., *J. Phys. Chem. A* 103:11328 (1999)
[11] Hughes, K.J., Blitz, M.A., Pilling, M.J., and Robertson, S.H., *Proc. Combust. Inst.* 29:2431-2437 (2002)
[12] Blitz, M.A., Hughes, K.J., Pillling, M., and Robertson, S.H., *J. Phys. Chem. A* 110:2996-3009 (2006)
[13] Baulch, D.L., Drysdale, D.D., Duxbury, J., and Grant, S.J., *Evaluated Data for High Temperature Reactions*, Butterworth, London, Vol. 3 (1976)
[14] Alzueta, M.U., Bilbao, R., and Glarborg, P., Combust. Flame 127:2234-2251 (2001)
[15] Hu, X. and Marshall, P., "Reactions of H/SO_2 Adducts with Atomic Hydrogen", poster presented at the 18th International Symposium on Gas Kinetics, Bristol, UK, August, 7-12, 2004
[16] Glarborg, P., Kubel, D., Dam–Johansen, K., Chiang, H.M., Bozzelli, J.W., *Int. J. Chem. Kinet.* 28:773–790 (1996)
[17] Blitz, M.A., Hughes, K.J., and Pilling, M.J., *J. Phys. Chem. A* 107:1971-1978 (2003)
[18] Marshall, P., unpublished
[19] Huber, K.P., and Herzberg, G.,"Molecular Spectra and Molecular Structure IV. Constants of Diatomic Molecules", Van Nostrand Reinhold, New York, 1979
[20] Sendt, K., Jazbec, M., and Haynes, B.S., *Proc. Combust. Inst.* 29:2439-2446 (2002)
[21] Blitz, M.A., McKee, K.W., and Pillling, M., *Proc. Combust. Inst.* 28:2491-2497 (2000)
[22] Tsuchiya, K., Kamiya, K., and Matsui, H., *Int. J. Chem. Kinet.* 29:57-66 (1997)
[23] Naidoo, J., Goumri, A., and Marshall, P., *Proc. Combust. Inst.* 30:1219-1225 (2005)
[24] Yilmaz, A., Hindiyarti, L., Jensen, A.D., Glarborg, P., and Marshall, P., "Thermal Dissociation of SO_3 at 1000-1400 K", *J. Phys. Chem. A*, in press (2005)
[25] Bacskay, G.B. and Mackie, J.C., *J. Phys. Chem. A* 109:2019-2025 (2005)
[26] Murakami, Y., Onishi, S., Kobayashi, T., Fujii, N., Ishiki, N., Tsuchiya, K., Tezaki, A., Matsui, H., *J. Phys. Chem. A* 107:10996-11000 (2003)
[27] Smith, O.I., Tseregounis, S., and Wang, S.–N., *Int. J. Chem. Kinet.* 14:679 (1982)
[28] Glarborg, P. and Marshall, P., *Combust. Flame* 141:22-38 (2004)
[29] Atkinson, R., Baulch, D.L., Cox, R.A., Hampson, R.F., Kerr, J.A., and Troe, J. *J. Phys. Chem. Ref. Data* 21:1125–1568 (1992)
[30] DeMore, W.B., Sander, S.P., Golden, D.M., Hampson, R.F., Kurylo, M.J., Howard, C.J., Ravishankara, A.R., Kolb, C.E., and Molina, M.J., "Chemical Kinetics and Photochemical Data for Use in Stratospheric Modeling. Evaluation Number 12", JPL Publication 97–4 (1997)
[31] Shiina, H., Miyoshi, A., and Matsui, H., *J. Phys. Chem. A* 102:3556-3559 (1998)
[32] Murakumi, Y., Onishi, S., and Fujii, N., *J. Phys. Chem. A* 108:8141-8144 (2004)
[33] Lovejoy, E.R., Wang, N.S., and Howard, C.J., *J. Phys. Chem.* 91:5749-5755 (1987)
[34] Wang, B., and Hou, H., *Chem. Phys. Lett.* 410:235-241 (2005)
[35] Lutz, A., Kee, R.J., and Miller, J.A., "SENKIN: A Fortran Program for Predicting Homogenous Gas Phase Chemical Kinetics with Sensitivity Analysis", Sandia Report SAND87–8248, Sandia National Laboratories, Livermore, CA (1987)
[36] Kee, R.J., Rupley, F.M., and Miller, J.A., "CHEMKIN–II: A Fortran Chemical Kinetics Package for the Analysis of Gas-Phase Chemical Kinetics", Sandia Report SAND89-8009, Sandia National Laboratories, Livermore, CA (1989)
[37] Mueller, M.A., Yetter, R.A., and Dryer, F.L., *Proc.*

Combust. Inst. 27:177 (1998)
[38] Cullis, C.F., and Mulcahy, M.R.F., *Combust. Flame* 18:225, (1972)

Table 1: Selected reactions from the H/S/O subset. Units are mol, cm, s, cal.

	Reaction	A	β	E_a	Reference
1.	$^3SO + H + M \rightleftharpoons HSO + M^a$	1.9×10^{20}	–1.31	662	[18]
2.	$^3SO + O(+M) \rightleftharpoons SO_2(+M^a)$	3.2×10^{13}	0.0	0	[14]
	Low pressure limit:	1.2×10^{21}	–1.54	0	
	Troe parameters: 0.55 10^{-30} 10^{30}				
3.	$^3SO + OH \rightleftharpoons SO_2 + H$	1.1×10^{17}	–1.35	0	[21]
4.	$^3SO + OH(+M) \rightleftharpoons HOSO(+M^a)$	1.6×10^{12}	0.50	–400	[10]
	Low pressure limit:	9.5×10^{27}	–3.48	970	
5.	$^3SO + O_2 \rightleftharpoons SO_2 + O$	7.6×10^{3}	2.37	2970	[22]
6.	$^3SO + HO_2 \rightleftharpoons SO_2 + OH$	3.7×10^{3}	2.42	7660	[18]
7.	$^1SO + M \rightleftharpoons {}^3SO + M$	1.0×10^{13}	0.0	0	est
8.	$^1SO + O_2 \rightleftharpoons SO_2 + O$	1.0×10^{13}	0.0	0	est
9.	$SO_2 + H(+M) \rightleftharpoons HOSO(+M^a)$	2.4×10^{8}	1.63	7340	[12]
	Low pressure limit:	1.8×10^{37}	–6.14	11070	
	Troe parameters: 0.283 272 3995				
10.	$SO_2 + H(+M) \rightleftharpoons HSO_2(+M^a)$	5.3×10^{8}	1.59	2470	[12]
	Low pressure limit:	1.4×10^{31}	–5.19	4510	
	Troe parameters: 0.390 167 2191				
11.	$SO_2 + O(+M) \rightleftharpoons SO_3(+M^a)$	3.7×10^{11}	0.0	1689	[23]
	Low pressure limit:	2.4×10^{27}	–3.60	5186	
	Troe parameters: 0.442 316 7442				
	$SO_2 + O(+N_2) \rightleftharpoons SO_3(+N_2)$	3.7×10^{11}	0.0	1689	[23, 24]
	Low pressure limit:	2.9×10^{27}	–3.58	5206	
	Troe parameters: 0.43 371 7442				
12.	$SO_2 + OH(+M) \rightleftharpoons HOSO_2(+M^a)$	5.7×10^{12}	–0.27	0	[17]
	Low pressure limit:	1.7×10^{27}	–4.09	0	
	Troe parameters: 0.10 10^{-30} 10^{30}				
13.	$SO_2 + CO \rightleftharpoons {}^3SO + CO_2$	1.9×10^{13}	0.0	65900	[25]
14.	$SO_2 + S \rightleftharpoons {}^3SO + {}^3SO$	6.0×10^{-16}	8.21	9600	[26]
15.	$SO_3 + H \rightleftharpoons SO_2 + OH$	5.5×10^{10}	0.99	3740	[18]
16.	$SO_2 + O \rightleftharpoons SO_2 + O_2$	7.8×10^{11}	0.0	6100	[24, 27]
17.	$SO_3 + {}^3SO \rightleftharpoons SO_2 + SO_2$	7.6×10^{3}	2.37	2980	[28]
18.	$HSO + H \rightleftharpoons {}^3SO + H_2$	1.0×10^{13}	0.0	0	est
19.	$HSO + H \rightleftharpoons SH + OH$	4.9×10^{19}	–1.86	1560	[16]
20.	$HSO + H \rightleftharpoons S + H_2O$	1.6×10^{9}	1.37	–340	[16]
21.	$HSO + O \rightleftharpoons SO_2 + H$	4.5×10^{14}	–0.40	0	[16]
22.	$HSO + O \rightleftharpoons {}^3SO + OH$	1.4×10^{13}	0.15	300	[16]
23.	$HSO + O_2 \rightleftharpoons HSO_2 + O$	8.4×10^{-7}	5.10	11312	[18]
24.	$HSO + OH \rightleftharpoons {}^3SO + H_2O$	1.7×10^{9}	1.03	470	[16]
25.	$HOSO(+M) \rightleftharpoons HSO_2(+M^a)$	1.0×10^{9}	1.03	50000	[10]
	Low pressure limit:	1.7×10^{35}	-5.64	55400	
	Troe parameters: 0.40 10^{-30} 10^{30}				
26.	$HOSO + H \rightleftharpoons {}^1SO + H_2O$	2.4×10^{14}	0.0	0	[15, 18]
27.	$HOSO + H \rightleftharpoons SO_2 + H_2$	1.8×10^{7}	1.72	–1286	[15, 18]
28.	$HOSO + O_2 \rightleftharpoons SO_2 + HO_2$	9.6×10^{1}	2.36	–10130	(T>800 K) [18]
29.	$HOSO + OH \rightleftharpoons SO_2 + H_2O$	6.0×10^{12}	0.0	0	est, see text
30.	$HSO_2 + H \rightleftharpoons SO_2 + H_2$	5.0×10^{12}	0.46	–262	[15, 18]
31.	$HSO_2 + O_2 \rightleftharpoons SO_2 + HO_2$	1.1×10^{3}	3.20	–235	[18]
32.	$HSO_2 + OH \rightleftharpoons SO_2 + H_2O$	1.0×10^{13}	0.0	0	est
33.	$HOSO_2 + O_2 \rightleftharpoons SO_3 + HO_2$	7.8×10^{11}	0.0	656	[29]
34.	$SH + O \rightleftharpoons {}^3SO + H$	1.0×10^{14}	0.0	0	[14]
35.	$S + OH \rightleftharpoons {}^3SO + H$	4.0×10^{13}	0.0	0	[30]
36.	$S + H_2 \rightleftharpoons SH + H$	1.4×10^{14}	0.0	19300	[31]

a: Enhanced third-body efficiencies: N_2=1.5, SO_2=10, H_2O=10, except for reactions (R9), (R10) where N_2=1.0; (R11), where N_2=0.0, and (R12), where N_2=1.0, SO_2=5, H_2O=5.

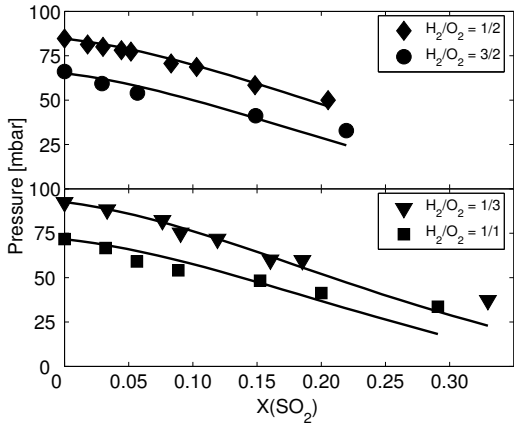

Fig. 1: Comparison between experimental data [8] and modeling predictions for the effect of SO_2 on the second pressure limit of explosion of H_2/O_2 mixtures in a batch reactor at 784 K. Initial conditions: Premixed $H_2/O_2/SO_2$ in specific ratios at a pressure greater than the second limit. Withdrawal of gases until explosion occurs. For modeling purpose, explosion must occur within 0.1 sec to account.

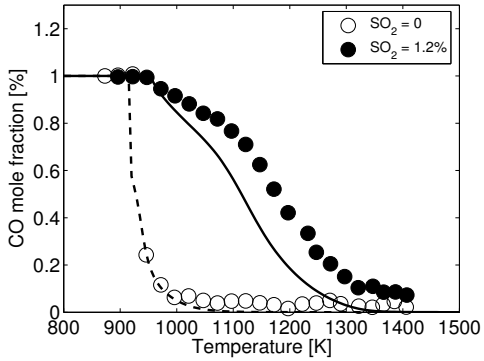

Fig. 2: Comparison between experimental data [9] and modeling predictions for the effect of SO_2 on the oxidation of CO/H_2 mixture under stoichiometric conditions in a flow reactor. Initial conditions: 1.0 % CO, 1.0 % H_2, 1.0 % O_2, 2.0 % H_2O, balance N_2, without and with 1.2 % SO_2. The residence time is 192/T.

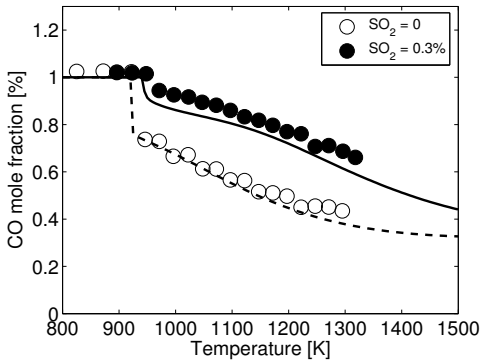

Fig. 3: Comparison between experimental data [9] and modeling predictions for the effect of SO_2 on the oxidation of CO/H_2 mixture under fuel-rich conditions in a flow reactor. Initial conditions: 1.0 % CO, 1.0 % H_2, 0.5 % O_2, 2.0 % H_2O, balance N_2, without and with 0.3 % SO_2. The residence time is 192/T.

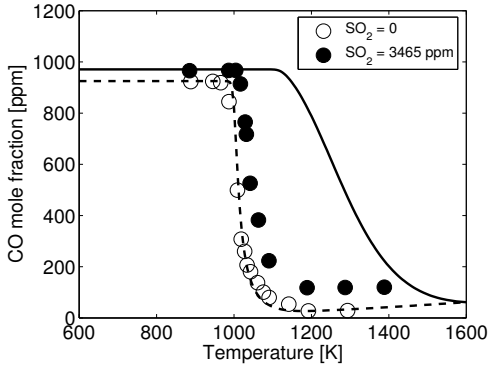

Fig. 4: Comparison between experimental data [14] and modeling predictions for the effect of SO_2 on the oxidation of CO in a flow reactor. Initial conditions without SO_2: 925 ppm CO, 260 ppm O_2, 2.0 % H_2O, balance N_2. The residence time is 200/T. Initial conditions with 3465 ppm SO_2: 971 ppm CO, 253 ppm O_2, 2.0 % H_2O, balance N_2. The residence time is 192/T.

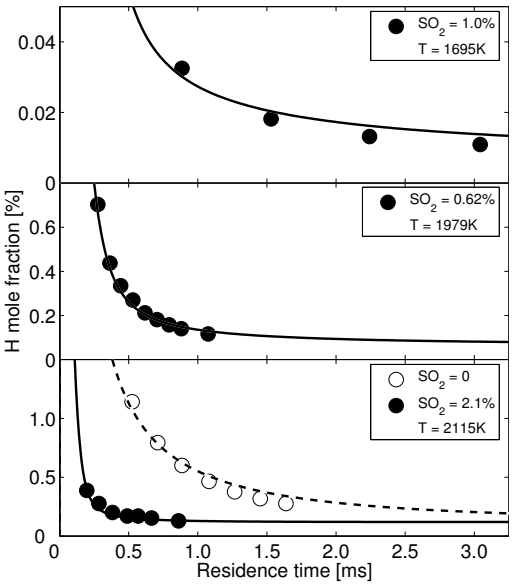

Fig. 5: Comparison between experimental data [5] and (plug flow) model predictions for the downstream H atom concentration in atmospheric pressure $H_2/O_2/N_2$ flames doped with SO_2. The calculated H atom profiles are shifted in time to match the experimental data at the largest gradient. Top: Feed composition $H_2/O_2/N_2$ = 4/1/6 with 1.0 % SO_2. Middle: Feed composition $H_2/O_2/N_2$ = 4/1/4 with 0.62 % SO_2. Bottom: Feed composition $H_2/O_2/N_2$ = 3/1/4 with no and 2.1 % SO_2, respectively. The listed temperature is the mean value of 2107 K and 2123 K for the undoped and doped flame, respectively.

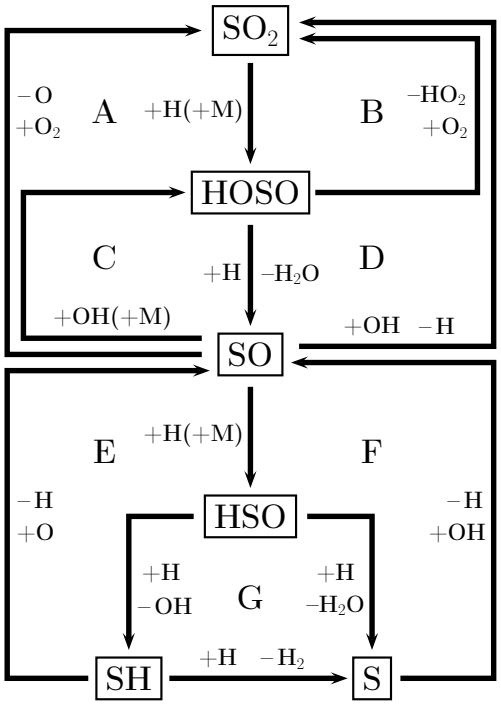

Fig. 6: Cyclic chain terminating sulphur sequences. Cycles are denoted by capital letters. The alphabetic order roughly reflects the important sequences at atmospheric pressure and increasing temperature from 1000 to 2000 K. The sum of each individual sequence yields (A): H+H+O_2⇌H_2O+O, (B): H+O_2⇌HO_2, (C,D,F): H+OH⇌H_2O, (E): H+O⇌OH, (G): H+H⇌H_2. In the diagram we have implicitly included a rapid intersystem crossing from singlet to triplet SO. Mechanism (G) differs from (F) by the intermediate conversion of HSO to SH before yielding S. Mechanism (B) is not truly chain terminating, but replaces a H atom with the less reactive HO_2 radical.